



Aerobic radical polymerization mediated by microbial metabolism

Gang Fan^{1,2}, Austin J. Graham^{1,2}, Jayaker Kolli¹, Nathaniel A. Lynd^{1,2} and Benjamin K. Keitz^{1,2}✉

Performing radical polymerizations under ambient conditions is a major challenge because molecular oxygen is an effective radical quencher. Here we show that the facultative electro-*gen Shewanella oneidensis* can control metal-catalysed living radical polymerizations under apparent aerobic conditions by first consuming dissolved oxygen via aerobic respiration, and then directing extracellular electron flux to a metal catalyst. In both open and closed containers, *S. oneidensis* enabled living radical polymerizations without requiring the removal of oxygen. Polymerization activity was closely tied to *S. oneidensis* anaerobic metabolism through specific extracellular electron transfer proteins and was effective for a variety of monomers using low (parts per million) concentrations of metal catalysts. Finally, polymerizations survived repeated challenges of oxygen exposure and could be initiated using lyophilized or spent (recycled) cells. Overall, our results demonstrate how the unique ability of *S. oneidensis* to use both oxygen and metals as respiratory electron acceptors can be leveraged to address salient challenges in polymer synthesis.

Radical-based reactions, which include radical polymerizations, are inhibited in the presence of molecular oxygen^{1,2}. Thus, controlled radical polymerizations require strictly anoxic conditions prior to initiation. Inspired by oxygen-consuming reactions in biology, several recent reports have shown that enzymatic reactions, such as the oxidation of β-D-glucose to D-glucono-δ-lactone via glucose oxidase, can rapidly deplete dissolved oxygen prior to reversible addition-fragmentation chain transfer^{3,4} and atom-transfer radical polymerization (ATRP)^{5–7}. Similarly, combinations of enzymes, such as glucose oxidase and horseradish peroxidase, can enable radical polymerizations that require the presence of oxygen to generate the radical initiator⁸. These and other recent advances allow some living radical polymerizations to be run in open containers under ambient conditions^{9–12}. However, the majority of polymerization methods that rely on in situ oxygen depletion require sacrificial reagents, produce strong oxidants, and/or are restricted to specific catalysts and monomers.

Given the inspiration behind the use of glucose oxidase, we predicted that whole-cell aerobic respiration could similarly deplete dissolved oxygen prior to initiating radical polymerization (Fig. 1). Towards this goal, we recently reported that the facultative electro-

gen *Shewanella oneidensis* (wild type, MR-1) can drive ATRP under anaerobic conditions by directing metabolic electron flux via its extracellular electron transfer (EET) machinery to Cu-based catalysts¹³. Given its respiratory plasticity, we hypothesized that *S. oneidensis* could metabolically control living radical polymerizations under ambient conditions by first consuming dissolved oxygen and then directing EET flux to a metal polymerization catalyst (Fig. 1). Here we demonstrate that *S. oneidensis* enables ATRP under aerobic conditions using a variety of monomers and metal catalysts at low (parts per million) concentrations. Aerobic polymerizations suppressed background radical reactions, could be run in open or shaking containers, and accentuated metabolic and genotypic differences between *S. oneidensis* strains. Finally, aerobic polymerizations produced homopolymers and block copolymers with well-controlled molecular weights at rates comparable to those of

other polymerization methodologies and could be initiated using lyophilized or spent cells. Overall, our results demonstrate how the unique metabolic capabilities of *S. oneidensis* effectively combine the advantages of enzymatic oxygen depletion and activator regenerated by electron transfer ATRP to yield well-defined synthetic polymers under ambient conditions.

Results

***S. oneidensis* consumes dissolved oxygen and activates EET flux to the metal polymerization catalyst.** To verify that *S. oneidensis* could create the anaerobic environment necessary for radical polymerization, we first measured dissolved oxygen depletion in *S. oneidensis* cultures under standard growth and polymerization conditions. In defined media (*Shewanella* basal medium (SBM); Supplementary Table 2) at an inoculation cell density of OD₆₀₀ = 0.2, *S. oneidensis* MR-1 growing on lactate consumed dissolved oxygen within minutes (Fig. 2a). Next, we examined oxygen consumption under typical polymerization conditions. We previously showed that polymerization mixtures that contained the monomer (oligo(ethylene oxide) methyl ether methacrylate-500 (OEOMA₅₀₀)), initiator (2-hydroxyethyl 2-bromoisobutyrate (HEBIB)), lactate as the primary carbon source, fumarate as the primary electron acceptor, and the metal catalyst (Cu(II)-TPMA (TPMA, tris(2-pyridylmethyl)amine)) inhibited bacterial growth, although cells remained viable¹³. Nevertheless, cultures that incorporated polymerization components also showed rapid oxygen depletion, albeit at a slower rate. Together, these results confirm that high densities of *S. oneidensis* cells quickly consume dissolved oxygen during growth in a defined media and under typical polymerization conditions.

Having confirmed that oxygen can be readily removed from *S. oneidensis* polymerization cultures, we next assessed the general feasibility of aerobic polymerizations. Below, aerobic conditions refer to polymerizations that use aerobically pregrown cells with no steps taken to remove oxygen. Anaerobic conditions refer to polymerizations that involve anaerobically pregrown cells performed in

¹McKetta Department of Chemical Engineering, University of Texas at Austin, Austin, TX, USA. ²Center for Dynamics and Control of Materials, University of Texas at Austin, Austin, TX, USA. ✉e-mail: keitz@utexas.edu

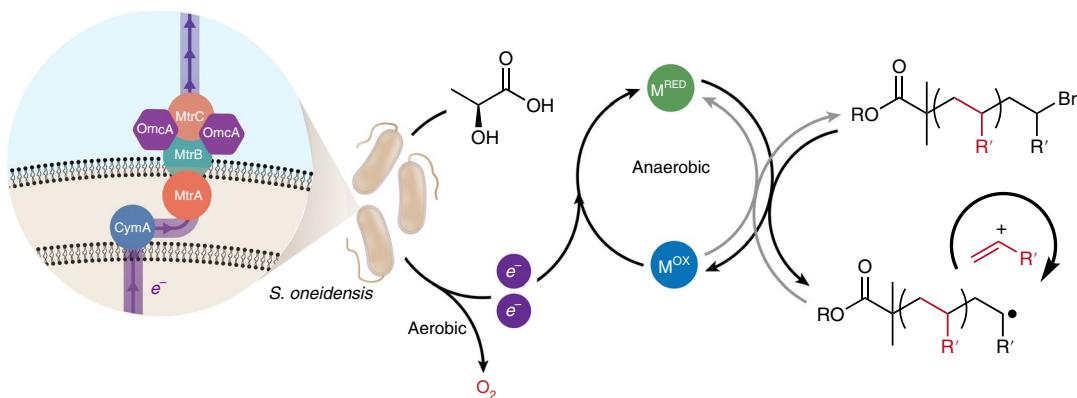


Fig. 1 | Carbon oxidation in *S. oneidensis* is coupled to either oxygen reduction under aerobic conditions or EET pathways under anaerobic conditions.

At high cell densities, dissolved oxygen is depleted to create an in situ anaerobic environment in which EET pathways are activated. Under anaerobic conditions, extracellular electron flux from the MtrCAB pathway in *S. oneidensis* MR-1 can be diverted to control the oxidation state of a transition metal polymerization catalyst through an atom-transfer radical polymerization mechanism. The polymerization rate and radical concentration are controlled by the equilibrium between oxidized (M^{OX}) and reduced (M^{RED}) metal catalyst.

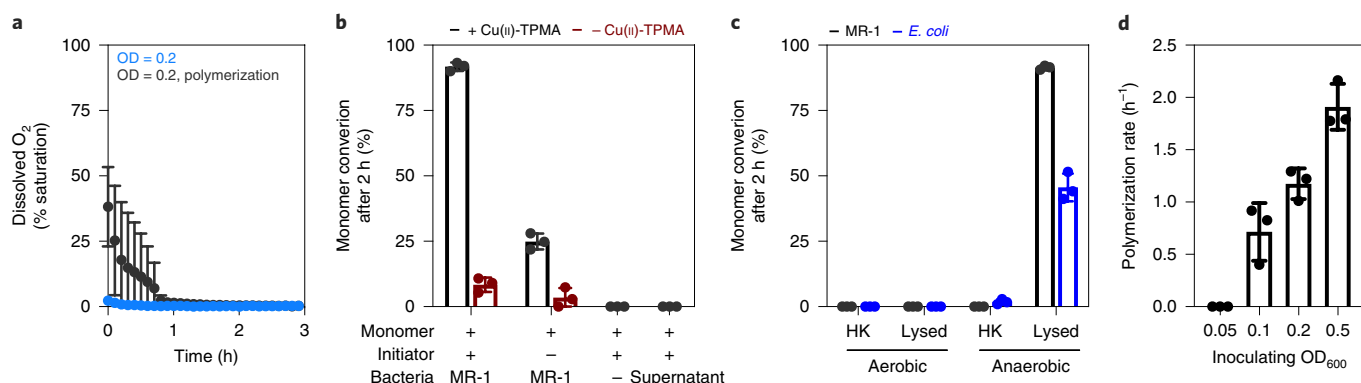


Fig. 2 | *S. oneidensis* rapidly consumes dissolved oxygen and activates radical polymerization in cultures for which no additional steps were taken to remove oxygen. **a**, Dissolved oxygen in *S. oneidensis* MR-1 cultures growing in SBM and under typical polymerization conditions. Under both conditions, oxygen consumption outcompetes oxygen diffusion. **b**, Effect of different biological and polymerization components on monomer ($OEOMA_{500}$) conversion under aerobic conditions. Monomer, initiator, catalyst, and *S. oneidensis* MR-1 are all required to achieve significant monomer conversion. **c**, Monomer ($OEOMA_{500}$) conversion using heat-killed (HK) and lysed *E. coli* MG1655 or *S. oneidensis* MR-1 cells under anaerobic and aerobic conditions. Lysed cells release intracellular reductants that reduce $Cu^{(II)}$ to $Cu^{(I)}$, which activates polymerization. Under aerobic conditions, adventitious reductants and radicals are quenched by oxygen. Heat-killed cells do not result in polymerization under either condition as they neither consume oxygen nor generate EET flux to reduce the metal catalyst. **d**, Polymerization rate constants of $OEOMA_{500}$ using *S. oneidensis* MR-1 and $Cu^{(II)}$ -TPMA at varying inoculating OD_{600} under aerobic conditions. Data show the mean \pm s.d. of $n=3$ replicates.

the absence of oxygen. In a typical polymerization reaction, *S. oneidensis* cells from stationary-phase pregrowth were inoculated into a polymerization mixture that contained monomer ($OEOMA_{500}$), initiator (HEBIB), lactate as the primary carbon source, fumarate as the primary anaerobic electron acceptor, and a metal catalyst (Cu -TPMA). In a closed vessel with no additional steps taken to remove oxygen, a polymerization mixture that contained aerobically pregrown *S. oneidensis* at an inoculation density of $OD_{600}=0.2$ showed near-quantitative monomer conversion (¹H NMR spectroscopy) after two hours. This result confirmed that polymerization was possible under ambient conditions, but we wanted to uncover the specific role of each reaction component. For example, we previously observed a catalyst-free background polymerization that proceeded to about 40% $OEOMA_{500}$ conversion over a 24-hour period under anaerobic conditions¹³. Under aerobic conditions, all polymerization components, including monomer, initiator, metal catalyst, and actively respiring *S. oneidensis* cells, were required for monomer conversion (Fig. 2b). Neglecting any of these components resulted

in substantially attenuated monomer conversion or no measurable activity in the case of *S. oneidensis* supernatant or cell-free negative controls. Although some background polymerization activity was observed in the absence of metal catalyst or initiator, these levels were lower than those under comparable anaerobic conditions¹³. During anaerobic polymerizations, we previously observed that lysed cells (both *S. oneidensis* MR-1 and *Escherichia coli* MG1655) could initiate substantial monomer conversion via the release of cytosolic reductants. In contrast, aerobic conditions suppressed background polymerization activity from lysed cells (Fig. 2c). These results show that in the absence of an active mechanism to remove dissolved oxygen (that is, aerobic respiration), initiation caused by adventitious radicals or uncontrolled reduction of the Cu catalyst is inhibited.

In general, aerobic polymerizations in sealed vessels exhibited first-order kinetics, suggesting effective control over radical concentration and allowing us to quantify polymerization rates (Supplementary Fig. 1). We measured the polymerization rates of

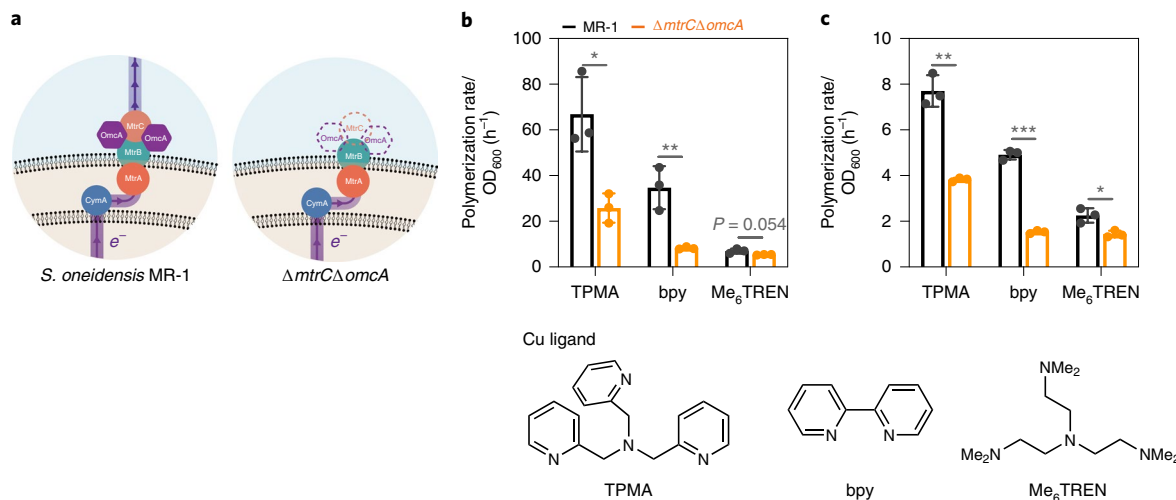


Fig. 3 | *S. oneidensis* strain and Cu(II/I) ligand control polymerization kinetics under anaerobic and aerobic conditions. **a**, Comparison of one EET pathway in *S. oneidensis* MR-1 and an EET-deficient knockout ($\Delta mtrC\Delta omcA$). **b,c**, Comparison of polymerization rate constants using *S. oneidensis* MR-1 or $\Delta mtrC\Delta omcA$ and different Cu ligands normalized by the initial cell inoculum in the polymerization mixture ($OD_{600}=0.02$ for anaerobic, panel **b**; $OD_{600}=0.2$ for aerobic, panel **c**). The $\Delta mtrC\Delta omcA$ strain consistently showed decreased polymerization rate relative to wild-type *S. oneidensis*, consistent with the reduced level of EET flux expected for this knockout. The metal ligand affects Cu redox potential, Cu(I) stability and overall polymerization activity. Data show the mean \pm SD of $n=3$ replicates. * $P < 0.05$, ** $P < 0.01$, *** $P < 0.001$.

OEOMA₅₀₀ under aerobic conditions as a function of starting inoculum size (OD_{600}) and found a linear dependence above a threshold of $OD_{600}=0.1$ (Fig. 2d). Below this cell population size, aerobic respiration can presumably not compensate for oxygen diffusion in order to create the anaerobic environment necessary for polymerization. Under anaerobic conditions (including pre-growth), polymerization rate was also proportional to the initial inoculum size and could be measured as low as $OD_{600}=0.004$ (Supplementary Fig. 1). Thus, when normalized to the initial cell population, aerobic polymerization rate constants were lower than those under anaerobic conditions, but still characteristic of a controlled polymerization. Notably, polymerizations run in completely open containers were also successful, with measured rate constants consistent with those of reactions in closed vessels (Supplementary Fig. 3). Furthermore, at higher cell densities, polymerizations were also tolerant to increased oxygen mass transfer, as indicated by successful polymerizations in tubes shaken at 100 r.p.m. (Supplementary Fig. 4). Overall, polymerization rate constants using Cu(II)-TPMA and *S. oneidensis* MR-1 under aerobic conditions were largely comparable to rates using glucose oxidase and horseradish peroxidase ($\sim 1.5\text{ h}^{-1}$ versus $0.56\text{--}5.9\text{ h}^{-1}$, respectively), but at lower catalyst concentrations ($\sim 20\text{ ppm}$ versus $100\text{--}1,000\text{ ppm}$ relative to monomer)⁶.

EET-controlled polymerization activity varies with metal catalyst and ligand environment. The polymerization rate of ATRP can be altered through the use of different Cu ligands or by using different metal catalysts. Under both aerobic and anaerobic conditions, we found that polymerization rate could be varied over several orders of magnitude by changing the ligand for Cu (Fig. 3b,c). Specifically, rates decreased in the order TPMA > bpy > Me₆TREN (bpy, 2,2'-bipyridine; Me₆TREN, tris(2-(dimethylamino)ethyl)amine). In an electrochemical cell under aqueous conditions, Me₆TREN previously displayed a faster polymerization rate than that of TPMA^{14–16}. Our results indicate that, in addition to affecting the reduction potential, deactivation rate and disproportionation propensity, the ligand environment around Cu may also influence its interaction with the EET machinery of *S. oneidensis*. Therefore, we examined the specific role of MtrC, one of the terminal reductases that allows *S. oneidensis* to use metals and metal oxides as

electron acceptors (Fig. 3a)^{17,18}. Consistent with our previous study, a *S. oneidensis* strain that lacked *mtrC* ($\Delta mtrC\Delta omcA$) showed significantly attenuated OEOMA₅₀₀ polymerization rates for all the Cu catalysts tested (Fig. 3b,c; Supplementary Fig. 5). Residual polymerization activity in the $\Delta mtrC\Delta omcA$ strain is most likely due to the presence of other EET pathways (that is, MtrDEF), which may also mediate Cu(II) reduction. Indeed, using OEOMA₃₀₀ as the monomer, additional *S. oneidensis* EET knockouts showed aerobic polymerization activity proportional to the number of cytochrome deletions (Supplementary Fig. 6). Together, these results highlight the extensive chemical (ligand structure) and biological (genotype) tools available to control polymerization activity under aerobic conditions.

As our polymerization is driven by EET flux to a metal catalyst, we predicted that other metals besides Cu should show appreciable polymerization activity under both anaerobic and aerobic conditions. Indeed, catalysts incorporating Fe (refs. 19,20), Co (refs. 21,22), Ni (refs. 23,24), and Ru (ref. 25) have all been reported to exhibit ATRP-like activity. Although alternative metal catalysts are generally less active than Cu, they are potentially advantageous due to their lower toxicity. Furthermore, many of these metals can support *S. oneidensis* growth or lie within the redox range of its outer membrane cytochromes^{17,26–28}. As predicted, we measured significant polymerization activity, relative to metal-free background controls, under anaerobic conditions for a variety of metal salts at low concentration (2 μ M) using ethylenediaminetetraacetic acid (EDTA) as the ligand (Fig. 4a). Similar to the case with Cu catalysts, the $\Delta mtrC\Delta omcA$ strain and *E. coli* MG1655 consistently showed reduced activity relative to *S. oneidensis* MR-1 for most of the metals tested (Supplementary Figs. 7–9). Next, we examined the activity of other metal complexes, which included cyanocobalamin, (Co(en)₃(NO₃)₃ (en, ethylenediamine), FeC₆H₅O₇ (citrate), (Ni(en)₃)Cl₂ and (Ru(bpy)₃)Cl₂ (Fig. 4b). With the exception of (Co(en)₃(NO₃)₃), all the complexes showed activity above background levels in the presence of *S. oneidensis* under anaerobic conditions. Subsequently, we measured the polymerization activity of several alternative metal catalysts under aerobic conditions. Only a handful of alternative metal catalysts at low concentration showed appreciable activity under these more challenging conditions, with

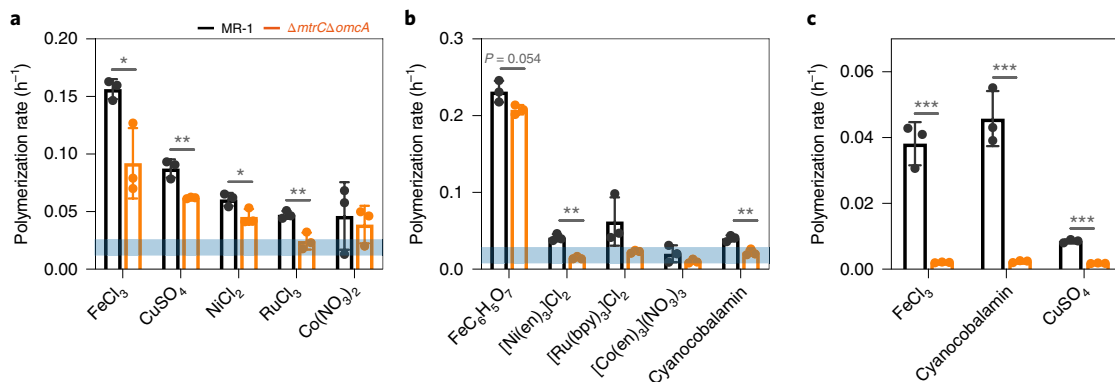


Fig. 4 | Radical polymerization was effective for a variety of metal catalysts in addition to Cu. **a**, Polymerization rate constants for different metal salts (2 μ M) with EDTA and different *S. oneidensis* strains (initial $OD_{600} = 0.02$) under anaerobic conditions. The horizontal blue bar represents an estimated rate constant for the metal-free background polymerization (Supplementary Fig. 8). **b**, Polymerization rate constants for different metal complexes (2 μ M) and *S. oneidensis* strains (initial $OD_{600} = 0.02$) under anaerobic conditions. **c**, Polymerization rate constants for different metal catalysts (2 μ M) and *S. oneidensis* strains (initial $OD_{600} = 0.2$) under aerobic conditions. Data show the mean \pm s.d. of $n=3$ replicates. * $P < 0.05$, ** $P < 0.01$, *** $P < 0.001$.

Table 1 | Monomer scope under anaerobic and aerobic polymerizations that involve *S. oneidensis* MR-1

Monomer	$\xrightarrow{\text{Cu-TPMA (10 } \mu\text{M)}}$ $\xrightarrow{\text{PEGIB}}$ $\xrightarrow{\text{S. oneidensis, } OD_{600} = 0.2}$ $\xrightarrow{30^\circ\text{C}}$						
	OEOMA_{300}	OEOMA_{500}	HEMA	MMA	DMAEMA	NIPAM	Styrene
Anaerobic							
OEOMA ₃₀₀	$82 \pm 10\%$ $172 \pm 8 \text{ kDa}$ $D = 1.40(5)$	$95 \pm 2\%$ $224 \pm 16 \text{ kDa}$ $D = 1.41(3)$	$86 \pm 2\%$ $120 \pm 24 \text{ kDa}$ $D = 1.30(8)$	$96 \pm 2\%$ $146 \pm 8 \text{ kDa}$ $D = 1.37(3)$	$83 \pm 4\%$ $403 \pm 31 \text{ kDa}$ $D = 1.15(1)$	$98 \pm 2\%$ $130 \pm 12 \text{ kDa}$ $D = 1.50(7)$	$14 \pm 2\%$ $556 \pm 122 \text{ kDa}$ $D = 1.59(8)$
Aerobic							
OEOMA ₅₀₀	$67 \pm 10\%$ $303 \pm 21 \text{ kDa}$ $D = 1.41(3)$	$96 \pm 2\%$ $191 \pm 10 \text{ kDa}$ $D = 1.36(2)$	$77 \pm 10\%$ $65 \pm 27 \text{ kDa}$ $D = 1.25(2)$	$8 \pm 3\%$ $233 \pm 130 \text{ kDa}$ $D = 1.32(22)$	—	$88 \pm 14\%$ $73 \pm 3 \text{ kDa}$ $D = 1.38(8)$	$11 \pm 1\%$ $290 \pm 104 \text{ kDa}$ $D = 1.76(54)$

Yields are listed as percentages, followed by experimental M_n and D . The target M_n values for the monomer:initiator of 500:1 were polyOEOMA₃₀₀ (150 kDa), polyOEOMA₅₀₀ (250 kDa), polyHEMA (651 kDa), polyNIPAM (56.6 kDa), polyDMAEMA (78.6 kDa), polyMMA (50.1 kDa) and PS (52.1 kDa). Average and s.d. values were obtained from $n=3$ replicates.

stark differences in polymerization rate between *S. oneidensis* MR-1 and the $\Delta mtrC\Delta omcA$ knockout (Fig. 4c). Consistent with previous reports^{19,20}, aerobic polymerization rates for FeCl_3 , cyanocobalamin and CuSO_4 were lower compared to those of optimized Cu-based catalysts. Although fewer metals were active under aerobic conditions, our results indicate that additional ligand optimization or increasing catalyst concentration could substantially improve activity, as was the case when Cu(II)-EDTA was replaced with Cu(II)-TPMA¹³.

EET-controlled polymerization is effective for a variety of monomers. Next, we evaluated the monomer scope and polymer properties under both anaerobic and aerobic conditions (Table 1). Cells were generally tolerant to many of the monomers tested, with minimal effects on viability (Supplementary Fig. 10). As a result, many of these monomers were amenable to microbial polymerization under both anaerobic and aerobic conditions. Even water-insoluble and toxic monomers, such as styrene²⁹, could be polymerized via

emulsion polymerization, albeit with a low yield (Supplementary Fig. 11). At low concentrations of Cu(II)-TPMA (2 μ M) and anaerobic conditions, theoretical molecular weights were substantially higher than predicted, probably due to inefficient initiation or catalyst deactivation (Supplementary Table 5). However, increasing the Cu concentration to 10 μ M (~100 ppm relative to monomer) and using a more water-soluble initiator (poly(ethylene glycol) methyl ether 2-bromoisoctyrate (PEGIB)) brought theoretical and predicted molecular weights into closer alignment, maintained narrow polydispersities, and had a minimal effect on cell viability (Table 1 and Supplementary Fig. 12). Overall, the trends in polymer molecular weight and polydispersity generally extended to aerobic conditions. For example, water-soluble monomers, which included OEOMA_{300/500}, (hydroxyethyl)methacrylate (HEMA) and *N*-isopropylacrylamide (NIPAM), yielded well-defined polymers near the targeted molecular weight under aerobic conditions. Gel permeation chromatography (GPC) traces for these polymers were also comparable to those from polymerizations conducted under

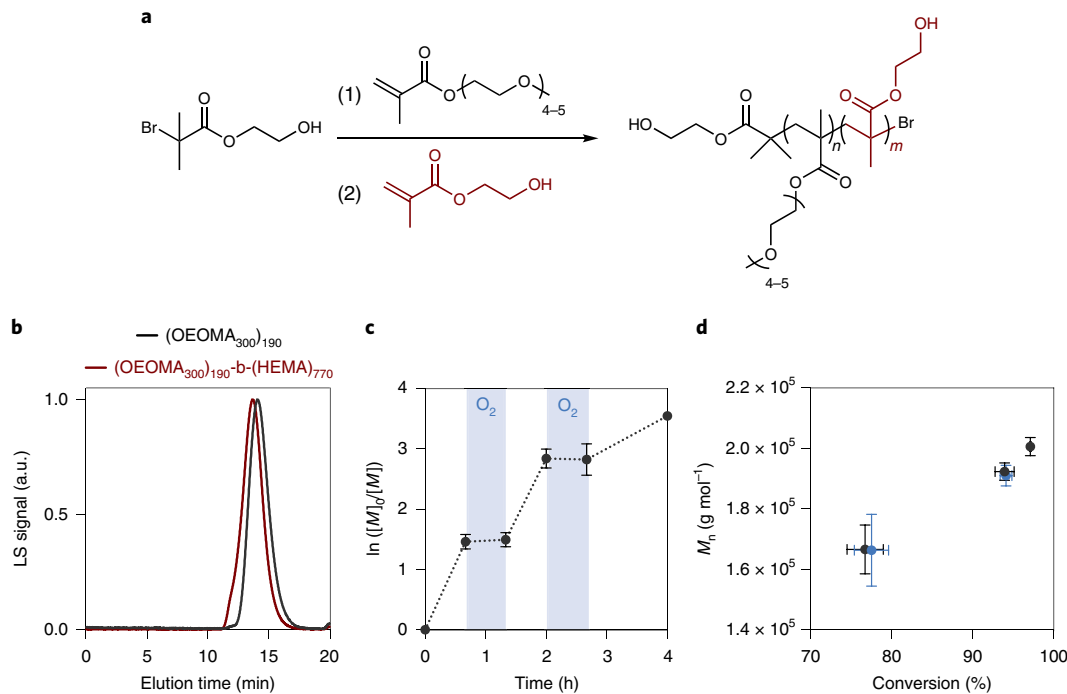


Fig. 5 | Aerobic *S. oneidensis* polymerizations can be used to prepare block copolymers and restarts automatically after multiple oxygen exposures.

a, Block copolymer of OEOMA₃₀₀ and HEMA synthesized under aerobic conditions with *S. oneidensis* MR-1. **b**, Gel permeation chromatograph of homopolymer and block copolymer. **c**, Polymerization kinetics in polymerization mixtures that contain *S. oneidensis* with and without oxygen bubbling. Polymerization stops during oxygen bubbling as the active Cu(i) catalyst is oxidized and the *S. oneidensis* EET pathways are downregulated. After bubbling ceases, the polymerization automatically restarts with a similar rate as EET flux reduces Cu(ii) to Cu(i). **d**, Molecular weight of poly(OEOMA₃₀₀) formed during the oxygen bubbling experiment. Blue points represent polymers isolated during oxygen (1.5 and 2.75 h) bubbling; black points represent polymers after the bubbling ceased (0.75, 2.25 and 4.25 h). The increase in molecular weight is consistent with polymerization restarting after oxygen bubbling stops. The data show mean \pm s.d. of $n=3$ replicates. LS, light scattering; a.u., arbitrary units.

anaerobic conditions (Supplementary Fig. 13). Polymer characteristics, such as polydispersity, were generally comparable to those of polymers prepared through traditional aqueous ATRP^{6,8}. Narrow polydispersity indices ($D \approx 1.1$) for poly(OEOMA₃₀₀) were also obtained when FeCl₃ and cyanocobalamin were used as the catalysts under aerobic conditions, although molecular weight was substantially higher than predicted (Supplementary Fig. 14). Finally, using Cu(ii)-TPMA and water-insoluble monomers, which included styrene and methyl methacrylate (MMA), yielded small amounts of polymer with non-ideal GPC traces under aerobic conditions. We attribute the performance of these monomers to a combination of poor solubility, the absence of surfactants in our media and cellular toxicity. Nevertheless, our results indicate that *S. oneidensis*-mediated polymerization is generally effective for a variety of monomers under both anaerobic and aerobic conditions.

Based on the range of different monomers amenable to polymerization, we next explored the synthesis of block copolymers (Fig. 5a). Using our standard aerobic conditions, OEOMA₃₀₀ was added to a polymerization mixture containing *S. oneidensis*. After 2 hours, a second monomer (HEMA) was added to form the block copolymer. GPC traces following polymer isolation revealed an increase in molecular weight relative to OEOMA₃₀₀ homopolymer and a final polydispersity index of 1.33 (Fig. 5b). Based on the success of block copolymer synthesis, we predicted that chain extension could also occur following exposure of the polymerization mixture to oxygen. Indeed, previous reports using enzymatic depletion of dissolved oxygen showed that polymerization can be stopped and restarted in the presence of oxygen⁸. Similarly, we found that aerating by bubbling air through a monomer-containing microbial

culture stopped polymerization, but that polymerization proceeded at similar rates when aeration ceased (Fig. 5c). The resumption of polymerization was also associated with increased polymer molecular weight (Fig. 5d, Supplementary Fig. 15). Together, these results demonstrate that our system can survive multiple oxygen challenges and can serve as a general platform for the synthesis of more advanced polymer architectures.

Polymerization activity is coupled to media formulation through *S. oneidensis* metabolism. We previously established that polymerization activity is dependent on EET flux, which can be altered using different carbon sources¹³. Under aerobic conditions, activity should also depend on cellular respiration as this consumes dissolved oxygen and is a prerequisite for radical propagation. Thus, to explore the relationship between cellular respiration and polymerization activity, we changed nutrient availability and employed different buffers. Consistent with the important role of functional metal reduction pathways, cells pregrown in media that lacked iron showed a reduced polymerization activity. Although we could not distinguish this effect from a general growth defect, it suggests that *S. oneidensis* was unable to obtain enough iron to construct functional components of the Mtr pathway (for example, haems) (Supplementary Fig. 16). Using anaerobically pregrown cells and polymerization conditions, the buffer had a minimal effect on the polymerization activity (Supplementary Fig. 17). During anaerobic growth, *S. oneidensis* expresses a proteome optimized for metal reduction, which includes the Mtr pathway^{26,30}. In contrast to our anaerobic results, aerobic polymerizations were highly dependent on the choice of microbial growth media (Supplementary Fig. 17).

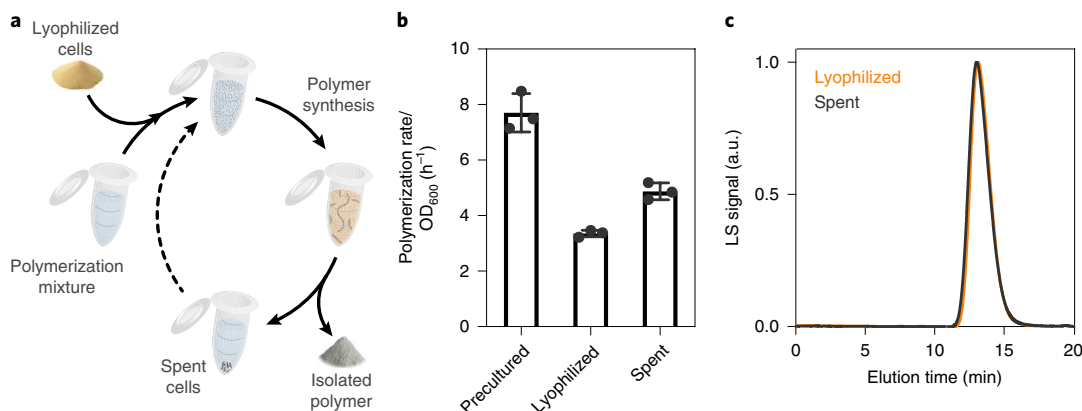


Fig. 6 | Aerobic polymerizations are effective using lyophilized and spent *S. oneidensis* cells. **a**, Reaction scheme for aerobic polymerizations using lyophilized and spent cells. Lyophilized cells were added to a polymerization mixture under aerobic conditions and sealed. After polymerization, the spent cells were collected via centrifugation, allowed to recover for 6 h in fresh media, then inoculated into a fresh polymerization mixture. **b**, Polymerization rate constants from precultured, lyophilized and spent *S. oneidensis* MR-1 cells. The normalized polymerization rates that involve lyophilized cells were lower because higher inoculating cell densities were required to account for cell death during lyophilization. **c**, GPC traces for poly(OEOMA₅₀₀) formed using lyophilized and spent cells. Unless otherwise indicated, data show the mean \pm s.d. of three replicates.

Polymerizations run in HEPES and PBS buffers showed reduced activity relative to SBM with casamino acids. We observed a similar decrease in aerobic polymerization rates when casamino acids were removed from SBM. Altogether, these results indicate that polymerization activity is closely coupled to aerobic and anaerobic respiratory pathways.

Lyophilized and spent cells can be employed as simple and regenerable polymerization reagents. A relative disadvantage of our aerobic polymerization is that it requires a preculturing step to obtain a sufficient density of *S. oneidensis* cells. To potentially streamline this protocol, we investigated whether lyophilized *S. oneidensis* cell powder could be directly added to an aerobic polymerization mixture (Fig. 6a). Using OEOMA₅₀₀ as the monomer, lyophilized cells showed comparable aerobic polymerization activity to that of precultured cells, but required a higher initial cell density (Fig. 6b). We also found that viable, spent cells could be collected from the polymerization mixture via centrifugation and reused for additional reactions after a short recovery period (~6 h) and supplying fresh reagents. Reactions conducted in this manner showed comparable polymerization kinetics and polymer properties to those using freshly cultured cells (Fig. 6c). Combined, these results demonstrate that our polymerization is effective without prior microbiology experience and that simple bioreactor designs, such as fermenters, could potentially be adapted for polymerization. Finally, the use of lyophilized cells and the ability to survive repeated challenges with oxygen highlight the robustness and potential scalability of our polymerization platform.

Discussion

We showed that *S. oneidensis* enables aerobic radical polymerizations by first consuming dissolved oxygen via aerobic respiration and then activating an ATRP catalyst through EET. Although a number of recent studies have performed radical polymerizations in the presence of living systems^{31–33}, our work demonstrates that microbial metabolism can be co-opted to rigorously control synthetic polymerizations under benchtop conditions. Furthermore, aerobic polymerizations that involve *S. oneidensis* compare favourably to alternative oxygen-tolerant polymerization methodologies. Photoredox catalysts (both organic and inorganic) are effective in organic solvents, but normally require small volumes and higher catalyst concentrations to account for oxygen depletion^{9,34}, although

ppm levels can be used in some cases³⁵. However, these systems are advantageous for monomers with poor aqueous solubility, such as styrene and MMA, and are not limited by the need for aqueous conditions. Enzymatic methods for in situ oxygen consumption are the most comparable to our platform as they are also generally confined to physiological temperatures and pH. As mentioned above, the use of glucose oxidase for oxygen depletion has been highly successful for both reversible addition–fragmentation chain transfer and ATRP, producing polymers with controlled molecular weights and narrow polydispersities^{3,4,6,8,11}. In contrast to our system, enzymatic polymerizations are not limited by potential concerns over cell viability. However, the direct production of hydrogen peroxide via glucose oxidase can be problematic for ATRP because the simultaneous presence of reduced metals can result in the creation of reactive oxygen species⁶. Thus, sacrificial reagents (that is, pyruvate) or additional enzymes are typically required to sequester hydrogen peroxide. Facultative bacteria, which include *S. oneidensis*, are specifically adapted to transition between aerobic and anaerobic environments. A carbon source is required for the polymerization, but this also contributes to biomass production and cellular respiration. Most importantly, the living nature of bacteria enables tunability and optimization through microbial engineering techniques (for example, metabolic pathway engineering, protein evolution, media optimization and so on) that is unavailable to other aerobic polymerization methods.

In general, we found that polymer molecular weight and polydispersity control using aerobic conditions, Cu-TPMA, and *S. oneidensis* MR-1 were comparable to those of polymers prepared using alternative aqueous ATRP strategies³⁶. A variety of monomers could be successfully polymerized and more advanced architectures, which include block copolymers, were also prepared. Polymer chain extension was also possible after challenging the culture with oxygen, which suggests our polymerizations are robust towards repeated oxygen exposure. These results are notable because there are a number of challenges inherent to aqueous ATRP, especially under aerobic conditions. As mentioned above, oxygen-tolerant ATRP using glucose oxidase produces reduced metals and strong oxidants, which can result in Fenton chemistry. Hydrogen peroxide is also a natural by-product of aerobic respiration. Indeed, *S. oneidensis* cultures produce hydrogen peroxide, especially after repeated transition from aerobic to anaerobic environments³⁷. We speculate that reactive oxygen species generated through these processes may

contribute to the relatively high polydispersities we measured for some monomers. Our initiator-free controls (Fig. 2b) allowed us to estimate the maximum potential contribution of uncontrolled polymerization as ~20% monomer conversion. Despite this, aerobic conditions eliminated a variety of other background polymerization processes relative to our previous anaerobic conditions. For example, we found that catalyst-free controls generated <10% monomer conversion under aerobic conditions, whereas ~40% conversion was observed under comparable anaerobic conditions¹³. Similarly, aerobic conditions eliminated polymerizations caused by the release of adventitious reductants during cell lysis. A variety of processes in addition to reactive oxygen species could further erode control over the polymerization. For example, *S. oneidensis* produces flavins³⁸, which exhibit polymerization activity upon light irradiation³⁹. In our previous work, we measured similar polymerization rates in *S. oneidensis* MR-1 and a flavin exporter knockout strain (Δbfe), which suggests that flavins are not significant contributors to polymerization activity¹³. However, we have not explored supplementation with exogenous flavins and the overall effect of flavins on background polymerization, as well as Cu(II) reduction, remains unexplored. Finally, free haem, as well as protein-bound haem (for example, haemoglobin) are also effective ATRP catalysts and may contribute to background polymerization in our system¹⁹. Thus, MtrC, which contains at least one solvent-exposed haem⁴⁰, could potentially catalyse polymerization in the absence of an exogenous metal catalyst. Overall, the substantial reduction of background processes in ambient conditions indicates that a controlled, continuous electron flux to the catalyst through EET is the predominant source of polymerization activity. Nevertheless, strategies that isolate and eliminate competing background radical polymerizations will be essential to improving the synthesis of well-defined polymers using *S. oneidensis*.

In addition to biological processes, the chemical mechanism of ATRP may also contribute to deviations from target molecular weights and narrow polydispersities. The equilibrium constant (K_{ATRP}) between Cu(I) and Cu(II) in water is particularly large, which accelerates the rate of polymerization, but can also lead to halide dissociation and early polymer chain termination^{16,41}. We observed this effect in our system at high optical densities ($OD_{600} \approx 0.2$; Supplementary Fig. 1) under anaerobic conditions in which a high EET flux presumably results in a large Cu(I) concentration that pushes K_{ATRP} even further towards Cu(II) and radical generation. This results in polymerization kinetics that deviate from first-order monomer conversion and prematurely cease due to chain-end termination. This result may also explain why fumarate is beneficial as the primary anaerobic electron acceptor. Our standard Cu(II) concentration (2–10 μ M) is too low to support anaerobic cell growth. Thus, the presence of fumarate ensures that *S. oneidensis* can readily transition from aerobic to anaerobic respiration while maintaining the metabolic flux necessary for polymerization. Aerobic polymerizations still occur in the absence of fumarate but are less controlled (Supplementary Fig. 18). We hypothesize that the loss of control occurs because a second function of fumarate is to divert respiratory flux from the EET pathways responsible for Cu(II) reduction. Reducing EET flux potentially decreases the concentration of Cu(I), K_{ATRP} and the frequency of side reactions that lead to chain-end termination. Thus, including fumarate results in a more controlled polymerization. To counteract the large aqueous K_{ATRP} , higher salt (NaCl, for example) concentrations are typically required in aqueous polymerizations, which include those performed with glucose oxidase, to suppress halide dissociation and chain termination. We did not include extra salts in our *S. oneidensis* polymerization cultures, but note that this species is halotolerant up to 0.2 M NaCl. This tolerance exceeds the NaCl concentrations (>10 mM) typically used in aqueous ATRP³⁶. Additionally, many *Shewanella* species are isolated from marine environments and readily tolerate increased

NaCl concentrations up to 2 M (refs. ^{42,43}), which makes salt addition a potentially viable strategy to increase polymerization control in our system. Finally, the use of less-active metals, which we showed exhibit some activity under aerobic conditions, may be another strategy to increase polymerization control.

Polymerization activity was highly dependent on both aerobic and anaerobic cellular metabolism. Specifically, we found that a critical population size ($OD_{600} \approx 0.1$) was necessary to counteract oxygen diffusion and enable radical polymerizations under aerobic conditions. Live cells also allowed polymerizations to survive repeated challenges with oxygen, which facilitated polymer chain extension even after oxygen exposure. In contrast, heat-killed cells showed no polymerization activity and *S. oneidensis* grown in non-optimal media or without casamino acids struggled to power aerobic polymerizations. This latter result is consistent with previous reports showing that the absence of casamino acids substantially attenuates the specific growth rate of *S. oneidensis*⁴⁴. Anaerobic respiration on Fe(III) in other *Shewanella* species is also slowed in the absence of these nutrients⁴⁵. Similarly, removing casamino acids from our system decreased the polymerization rate under completely anaerobic conditions (Supplementary Fig. 17), but the effect was not as dramatic as under aerobic conditions. If growth rate and respiration are impaired, it is likely that aerobic respiration cannot compete effectively with oxygen diffusion to create the anaerobic environment required for polymerization. This is particularly problematic with monomers that negatively impact cell viability, as these may further impede respiration. As aerobic polymerizations depend on the consumption of dissolved oxygen, we speculate that additional media-related polymerization activity differences are tied to the *S. oneidensis* growth rate and relative flux through the tricarboxylic acid cycle. Under ideal aerobic conditions growing on lactate, *S. oneidensis* diverts a substantial fraction of metabolic carbon flux (~50%) to the build-up of intermediates, such as pyruvate and acetate^{46,47}. Similar to *E. coli*, the inclusion of casamino acids and other nutrients may augment biomass synthesis and allow *S. oneidensis* cells to devote more resources to bioenergy generation via respiration, in addition to increasing their specific growth rate⁴⁸. In our system, this translates to improved oxygen consumption and polymerization rates. As our polymerization simultaneously leverages both aerobic and anaerobic metabolism, tuning these pathways in *S. oneidensis* could be used to further optimize polymerization activity^{49,50}.

Manipulating aerobic respiration rates in *E. coli* and other organisms to control dissolved oxygen has been an important focus of metabolic engineering⁵⁰. Applying similar strategies to *S. oneidensis* could expand the functional range of aerobic radical polymerizations by improving oxygen consumption rates. Once an anaerobic microenvironment was created, we showed that polymerization activity is governed by EET flux through the Mtr pathway. For example, we demonstrated that aerobic polymerization activity in *S. oneidensis* cultures is also dependent on the presence of the Mtr electron-transfer pathway. A strain that lacks MtrC and OmcA ($\Delta mtrC\Delta omcA$) displayed attenuated polymerization activity and additional Mtr knockouts showed further reductions in polymerization rate, which suggests that MtrF is also an important contributor to Cu(II) reduction. Together, these results indicate that *S. oneidensis* controls polymerization by influencing the concentration of Cu(I) and K_{ATRP} via the expression of specific EET proteins. Thus, an alternative strategy to lower K_{ATRP} and achieve better polymerization control is to regulate EET flux through the controlled expression of Mtr pathway components. EET flux can also be manipulated in other ways, such as by removing hydrogenases⁵¹, overexpressing flavins⁵², or changing carbon sources. Similar to their application in microbial fuel cells, these strategies could be employed to increase or decrease EET flux to the metal catalyst over competing pathways. We previously showed that the carbon source

for *S. oneidensis* impacts the polymerization rate under anaerobic conditions¹³. In this study, we used lactate in polymerization cultures that involve *S. oneidensis*, but note that it can be transformed to metabolize glucose and other inexpensive carbon sources⁵³. Alternatively, other facultative hosts that contain both aerobic and EET pathways, such as different *Shewanella* species, Mtr-expressing *E. coli*, or *Vibrio natriegens*, could be used in place of *S. oneidensis* to affect aerobic polymerizations^{54–56}. Although our platform is potentially amenable to extensive optimization via metabolic engineering, the effectiveness of lyophilized and spent cells demonstrates its simplicity and reusability.

Overall, we showed that *S. oneidensis* enables aerobic radical polymerizations by consuming dissolved oxygen and then activating an ATRP catalyst through its EET pathways. Polymerization was well-controlled, effective for a variety of monomers and metal catalysts, and could withstand repeated oxygen challenges. Finally, polymerization could be initiated using lyophilized *S. oneidensis* cells, which improved the accessibility of our polymerization. Among electrogenic bacteria, *S. oneidensis* is unusual in that extracellular metal reduction is coupled to substrate-level phosphorylation to support cell growth⁵⁷. Our results demonstrate how this unique hybrid of respiratory and fermentative metabolism, along with the facultative nature of *S. oneidensis*, can be used to address challenges in polymer synthesis and expand the synthetic capabilities of biological systems.

Materials

General polymerization conditions. Prior to polymerizations, stock solutions of HEBIB (2.9 µl in 26.1 µl of SBM that contained casamino acids) and Cu-TPMA (200× stock from 8.9 mg of CuBr₂ and 11.6 mg of TPMA per 100 ml of DMF) were prepared. Afterwards, a 1 ml polymerization reaction mixture was prepared as follows. In a sterile polypropylene culture tube, 60% w/w sodium lactate solution (2.85 µl), 1 M fumarate solution (40 µl), OEOMA₃₀₀ (28.6 µl), HEBIB (1.45 µl of stock solution), Cu-TPMA (5 µl of 200× DMF stock) and a balance of SBM with casamino acids, but lacking trace mineral mix, were mixed. Final concentrations were lactate (20 mM), fumarate (40 mM), monomer (100 mM), HEBIB (1 mM) and Cu-TPMA (2 µM). Polymerization was initiated by adding 10 µl of 100× cell stock (OD₆₀₀ = 2.0 for anaerobic, OD₆₀₀ = 20 for aerobic) to bring the final reaction volume to 1 ml and starting bacterial OD₆₀₀ to 0.02 (anaerobic) or 0.2 (aerobic). The final reaction mixtures were incubated at 30 °C (*S. oneidensis*) or 37 °C (*E. coli*). Time points were aliquoted, diluted with deuterium oxide or GPC solvents and then flash frozen in liquid N₂. Aliquots were stored at -20 °C until analysis via NMR spectroscopy or GPC. Prior to GPC measurement, cells were spun down at 6,000g from the water-soluble polymer solution. The polymer sample was loaded into dialysis tubing (MW cutoff, 1,000–3,000 Da) in the corresponding dialysis buffer. After dialyzing for 2 h, the buffer was replaced with fresh dialysis buffer and stirred overnight. Finally, the sample was removed from the dialysis bag, frozen at -80 °C overnight and then lyophilized.

Online content

Any Nature Research reporting summaries, source data, extended data, supplementary information, acknowledgements, peer review information; details of author contributions and competing interests; and statements of data and code availability are available at <https://doi.org/10.1038/s41557-020-0460-1>.

Received: 25 April 2019; Accepted: 23 March 2020;

Published online: 18 May 2020

References

1. Matyjaszewski, K., Coca, S., Gaynor, S. G., Wei, M. & Woodworth, B. E. Controlled radical polymerization in the presence of oxygen. *Macromolecules* **31**, 5967–5969 (1998).
2. Matyjaszewski, K., Patten, T. E. & Xia, J. Controlled 'living' radical polymerization. Kinetics of the homogeneous atom transfer radical polymerization of styrene. *J. Am. Chem. Soc.* **119**, 674–680 (1997).
3. Chapman, R., Gormley, A. J., Herpoldt, K.-L. & Stevens, M. Highly controlled open vessel RAFT polymerizations by enzyme degassing. *Macromolecules* **47**, 8541–8547 (2014).
4. Chapman, R., Gormley, A. J., Stenzel, M. H. & Stevens, M. Combinatorial low-volume synthesis of well-defined polymers by enzyme degassing. *Angew. Chem. Int. Ed.* **128**, 4576–4579 (2016).
5. Oytun, F., Kahveci, M. U. & Yagci, Y. Sugar overcomes oxygen inhibition in photoinitiated free radical polymerization. *J. Polym. Sci. A* **51**, 1685–1689 (2013).
6. Enciso, A. E., Fu, L., Russell, A. J. & Matyjaszewski, K. A breathing atom-transfer radical polymerization: fully oxygen-tolerant polymerization inspired by aerobic respiration of cells. *Angew. Chem. Int. Ed.* **57**, 933–936 (2018).
7. Wang, Y., Fu, L. & Matyjaszewski, K. Enzyme-deoxygenated low parts per million atom transfer radical polymerization in miniemulsion and ab initio emulsion. *ACS Macro Lett.* **7**, 1317–1321 (2018).
8. Enciso, A. E. et al. Biocatalytic 'oxygen-fueled' atom transfer radical polymerization. *Angew. Chem. Int. Ed.* **57**, 16157–16161 (2018).
9. Pester, C. W. et al. Engineering surfaces through sequential stop-flow photopatterning. *Adv. Mater.* **28**, 9292–9300 (2016).
10. Narupai, B. et al. Simultaneous preparation of multiple polymer brushes under ambient conditions using microliter volumes. *Angew. Chem. Int. Ed.* **57**, 13433–13438 (2018).
11. Gormley, A. J. et al. An oxygen-tolerant PET-RAFT polymerization for screening structure–activity relationships. *Angew. Chem. Int. Ed.* **57**, 1557–1562 (2018).
12. Yeow, J., Chapman, R., Gormley, A. J. & Boyer, C. Up in the air: oxygen tolerance in controlled/living radical polymerisation. *Chem. Soc. Rev.* **47**, 4357–4387 (2018).
13. Fan, G., Dundas, C., Graham, A. J., Lynd, N. A. & Keitz, B. K. *Shewanella oneidensis* as a living electrode for controlled radical polymerization. *Proc. Natl Acad. Sci. USA* **115**, 4559–4564 (2018).
14. Tang, W. & Matyjaszewski, K. Effect of ligand structure on activation rate constants in ATRP. *Macromolecules* **39**, 4953–4959 (2006).
15. Chmielarz, P., Park, S., Simakova, A. & Matyjaszewski, K. Electrochemically mediated ATRP of acrylamides in water. *Polymer* **60**, 302–307 (2015).
16. Fantic, M., Isse, A. A., Gennaro, A. & Matyjaszewski, K. Understanding the fundamentals of aqueous ATRP and defining conditions for better control. *Macromolecules* **48**, 6862–6875 (2015).
17. Breuer, M., Rosso, K. M. & Blumberger, J. Electron flow in multiheme bacterial cytochromes is a balancing act between heme electronic interaction and redox potentials. *Proc. Natl Acad. Sci. USA* **111**, 611–616 (2014).
18. Shi, L. et al. Extracellular electron transfer mechanisms between microorganisms and minerals. *Nat. Rev. Microbiol.* **14**, 651–662 (2016).
19. Silva, T. B. et al. Hemoglobin and red blood cells catalyze atom transfer radical polymerization. *Biomacromolecules* **14**, 2703–2712 (2013).
20. Simakova, A., Mackenzie, M., Averick, S. E., Park, S. & Matyjaszewski, K. Bioinspired iron-based catalyst for atom transfer radical polymerization. *Angew. Chem. Int. Ed.* **52**, 12148–12151 (2013).
21. Debuigne, A., Poli, R., Jérôme, C., Jérôme, R. & Detrembleur, C. Overview of cobalt-mediated radical polymerization: roots, state of the art and future prospects. *Prog. Polym. Sci.* **34**, 211–239 (2009).
22. Peng, C.-H., Yang, T.-Y., Zhao, Y. & Fu, X. Reversible deactivation radical polymerization mediated by cobalt complexes: recent progress and perspectives. *Org. Biomol. Chem.* **12**, 8580–8587 (2014).
23. Granel, C., Dubois, J., Jérôme, R. & Teyssié, P. Controlled radical polymerization of methacrylic monomers in the presence of a bis(ortho-chelated) arylnickel(II) complex and different activated alkyl halides. *Macromolecules* **29**, 8576–8582 (1996).
24. Uegaki, H., Kotani, Y., Kamigaito, M. & Sawamoto, M. Nickel-mediated living radical polymerization of methyl methacrylate. *Macromolecules* **30**, 2249–2253 (1997).
25. Ouchi, M., Yoda, H., Terashima, T. & Sawamoto, M. Aqueous metal-catalyzed living radical polymerization: highly active water-assisted catalysis. *Polym. J.* **44**, 51–58 (2011).
26. Beliaev, A. et al. Global transcriptome analysis of *Shewanella oneidensis* MR-1 exposed to different terminal electron acceptors. *J. Bacteriol.* **187**, 7138–7145 (2005).
27. Workman, D. J., Woods, S. L., Gorby, Y. A., Fredrickson, J. K. & Truex, M. J. Microbial reduction of vitamin B₁₂ by *Shewanella alga* strain BrY with subsequent transformation of carbon tetrachloride. *Environ. Sci. Technol.* **31**, 2292–2297 (1997).
28. Amonette, J. E., Workman, D. J., Kennedy, D. W., Fruchter, J. S. & Gorby, Y. A. Dechlorination of carbon tetrachloride by Fe(II) associated with goethite. *Environ. Sci. Technol.* **34**, 4606–4613 (2000).
29. McKenna, R. & Nielsen, D. R. Styrene biosynthesis from glucose by engineered *E. coli*. *Metab. Eng.* **13**, 544–554 (2011).

30. Kasai, T., Kouzuma, A., Nojiri, H. & Watanabe, K. Transcriptional mechanisms for differential expression of outer membrane cytochrome genes *omcA* and *mtrC* in *Shewanella oneidensis* MR-1. *BMC Microbiol.* **15**, 68 (2015).

31. Geng, J. et al. Radical polymerization inside living cells. *Nat. Chem.* **11**, 578–586 (2019).

32. Niu, J. et al. Engineering live cell surfaces with functional polymers via cytocompatible controlled radical polymerization. *Nat. Chem.* **9**, 537–545 (2017).

33. Romero, G. et al. Protective polymer coatings for high-throughput, high-purity cellular isolation. *ACS Appl. Mater. Inter.* **7**, 17598–17602 (2015).

34. McCarthy, B. & Miyake, G. M. Organocatalyzed atom transfer radical polymerization catalyzed by core modified N-aryl phenoxazines performed under air. *ACS Macro. Lett.* **7**, 1016–1021 (2018).

35. Corrigan, N., Rosli, D., Jones, J., Xu, J. & Boyer, C. Oxygen tolerance in living radical polymerization: investigation of mechanism and implementation in continuous flow polymerization. *Macromolecules* **49**, 6779–6789 (2016).

36. Simakova, A., Averick, S. E., Konkolewicz, D. & Matyjaszewski, K. Aqueous ARGET ATRP. *Macromolecules* **45**, 6371–6379 (2012).

37. Sekar, R. & DiChristina, T. J. Microbially driven Fenton reaction for degradation of the widespread environmental contaminant 1,4-dioxane. *Environ. Sci. Technol.* **48**, 12858–12867 (2014).

38. Kotloski, N. J. & Gralnick, J. A. Flavin electron shuttles dominate extracellular electron transfer by *Shewanella oneidensis*. *mBio* **4**, e00553–12 (2013).

39. Batchelor, R., Kwandou, G., Spicer, P. & Stenzel, M. (–)-Riboflavin (vitamin B2) and flavin mononucleotide as visible light photo initiators in the thiol–ene polymerisation of PEG-based hydrogels. *Polym. Chem.* **8**, 980–984 (2017).

40. Edwards, M., White, G. & Norman, M. Redox linked flavin sites in extracellular decaheme proteins involved in microbe–mineral electron transfer. *Sci. Rep.* **5**, 11677 (2015).

41. Ribelli, T. G., Lorandi, F., Fantin, M. & Matyjaszewski, K. Atom transfer radical polymerization: billion times more active catalysts and new initiation systems. *Macromol. Rapid Comm.* **40**, e1800616 (2019).

42. Hau, H. H. & Gralnick, J. A. Ecology and biotechnology of the genus *Shewanella*. *Annu. Rev. Microbiol.* **61**, 237–258 (2007).

43. Venkateswaran, K. et al. Polyphasic taxonomy of the genus *Shewanella* and description of *Shewanella oneidensis* sp. nov. *Int. J. Syst. Evol. Microbiol.* **49**, 705–724 (1999).

44. Tang, Y. J. et al. Invariability of central metabolic flux distribution in *Shewanella oneidensis* MR-1 under environmental or genetic perturbations. *Biotechnol. Prog.* **25**, 1254–1259 (2009).

45. Lovley, D., Phillips, E. & Lonergan, D. Hydrogen and formate oxidation coupled to dissimilatory reduction of iron or manganese by *Alteromonas putrefaciens*. *Appl. Environ. Microbiol.* **55**, 700–706 (1989).

46. Feng, X., Xu, Y., Chen, Y. & Tang, Y. J. Integrating flux balance analysis into kinetic models to decipher the dynamic metabolism of *Shewanella oneidensis* MR-1. *PLoS Comput. Biol.* **8**, e1002376–12 (2012).

47. Ishiki, K. & Shiigi, H. Kinetics of intracellular electron generation in *Shewanella oneidensis* MR-1. *Anal. Chem.* **91**, 14401–14406.

48. Basan, M. et al. Overflow metabolism in *Escherichia coli* results from efficient proteome allocation. *Nature* **528**, 99–104 (2015).

49. Veit, A., Polen, T. & Wendisch, V. F. Global gene expression analysis of glucose overflow metabolism in *Escherichia coli* and reduction of aerobic acetate formation. *Appl. Microbiol. Biotechnol.* **74**, 406–421 (2006).

50. Zhu, J., Sánchez, A., Bennett, G. N. & San, K.-Y. Manipulating respiratory levels in *Escherichia coli* for aerobic formation of reduced chemical products. *Metab. Eng.* **13**, 704–712 (2011).

51. Joshi, K., Kane, A. L., Kotloski, N. J., Gralnick, J. A. & Bond, D. R. Preventing hydrogen disposal increases electrode utilization efficiency by *Shewanella oneidensis*. *Front. Energy Res.* **7**, 95 (2019).

52. Yang, Y. et al. Enhancing bidirectional electron transfer of *Shewanella oneidensis* by a synthetic flavin pathway. *ACS Synth. Biol.* **4**, 815–823 (2015).

53. Choi, D. et al. Metabolically engineered glucose-utilizing *Shewanella* strains under anaerobic conditions. *Bioresource Technol.* **154**, 59–66 (2014).

54. Jensen, H. M. et al. Engineering of a synthetic electron conduit in living cells. *Proc. Natl Acad. Sci. USA* **107**, 19213–19218 (2010).

55. Jensen, H. M., TerAvest, M. A., Kokish, M. G. & Ajo-Franklin, C. M. CymA and exogenous flavins improve extracellular electron transfer and couple it to cell growth in Mtr-expressing *Escherichia coli*. *ACS Synth. Biol.* **5**, 679–688 (2016).

56. Long, C. P., Gonzalez, J. E., Cipolla, R. M. & Antoniewicz, M. R. Metabolism of the fast-growing bacterium *Vibrio natriegens* elucidated by ¹³C metabolic flux analysis. *Metab. Eng.* **44**, 191–197 (2017).

57. Hunt, K., Flynn, J., Naranjo, B., Shikhare, I. & Gralnick, J. Substrate-level phosphorylation is the primary source of energy conservation during anaerobic respiration of *Shewanella oneidensis* strain MR-1. *J. Bacteriol.* **192**, 3345–3351 (2010).

Publisher's note Springer Nature remains neutral with regard to jurisdictional claims in published maps and institutional affiliations.

© The Author(s), under exclusive licence to Springer Nature Limited 2020

Data availability

Raw data supporting the findings in this study are available through the Texas Data Repository (<https://doi.org/10.18738/T8/KHF1AY>).

Acknowledgements

We thank G. Bora, J. Imbrogno, M. Chwatko and J. Wagner for their experimental assistance. *S. oneidensis* knockouts were a generous gift from J. Gralnick. A.J.G. was supported through a National Science Foundation Graduate Research Fellowship (Program Award no. DGE-1610403). J.K. was supported through the Welch Foundation (Grant H-F-0001) during the Welch Summer Scholars Program. We gratefully acknowledge the use of facilities within the core microscopy lab of the Institute for Cellular and Molecular Biology, University of Texas at Austin. H. Alper is thanked for the use of a BioLector Pro. The research reported in this publication was supported by the National Institute of General Medical Sciences of the National Institutes of Health under Award no. R35GM133640. The content is solely the responsibility of the authors and does not necessarily represent the official views of the National Institutes of Health. Additional research support was provided by the Welch Foundation (Grants F-1929 and F-1904) and by the National Science Foundation through the Center for Dynamics and Control of Materials—an NSF Materials Research Science and Engineering Center

under Cooperative Agreement DMR- 1720595. NMR spectra were collected on a Bruker Avance III 500 funded by the NIH (Award 1 S10 OD021508-01) and a Bruker Avance III HD 400 funded by the NSF (Award CHE 1626211).

Author contributions

G.F., A.J.G., N.A.L. and B.K.K. designed the research; G.F., A.J.G. and J.K. performed the research; N.A.L. contributed new reagents and analytic tools; G.F., A.J.G., N.A.L. and B.K.K. analysed the data and wrote the paper.

Competing interests

The authors declare no competing interests.

Additional information

Supplementary information is available for this paper at <https://doi.org/10.1038/s41557-020-0460-1>.

Correspondence and requests for materials should be addressed to B.K.K.

Reprints and permissions information is available at www.nature.com/reprints.